An Electrodynamic Vacuum Arc Ion Acceleration Mechanism Based on Ampere's Force Law

Neal Graneau

Abstract—**The role of electrodynamic theory in vacuum arc processes has long been recognized in some aspects of modern theory and design of vacuum interrupters, and almost completely ignored in others. For example, it is well known that the motion of cathode spots is of electromagnetic origin, thus leading to methods of steering the spots by controlling the direction of the self and applied magnetic fields [1].**

However, the work presented here primarily involves the ion flux from the cathode spot. There are two well-recognized features of this flux that are very striking, and both have proved to be difficult to explain. These are the anomalously high energies of the ions, and their highly anisotropic spatial distribution. An electrodynamic acceleration mechanism based on Ampere's force law is proposed as an explanation to these phenomena. This theory is shown to be consistent with existing particle production models, and also provides a consistent solution to macroparticle emission and retrograde motion.

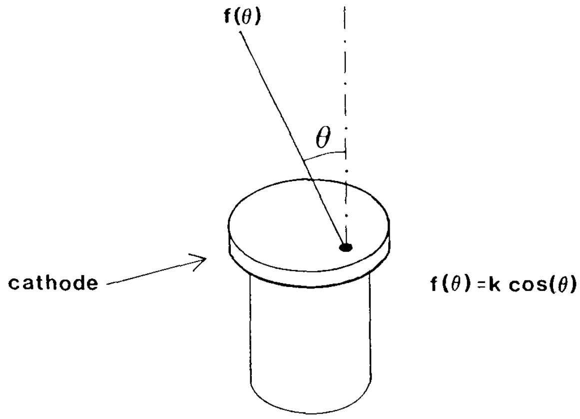

Fig. 1. Angle convention used to discuss ion flux from a cathode spot.

I. Previously Confirmed Experimental Results

THE first detection of what we now call the ion jet was made by Tanberg [2]. He measured the jet itself with a small vane mounted above the cathode spot. He also measured the reaction force pressing onto the cathode surface, and thus deduced that there was a "vapor stream" being ejected from copper cathode spots with velocities of the order of 10^4 m/s. The original explanation of this phenomenon was thermal, with a deduced spot temperature of 500,000 K. However the more common concept that existed until the 1960's [3], [4] was that the jet was caused by the magnetic pinch effect just above the cathode spot. Although this theory seems to lend itself to an explanation of the anisotropic ion flux, it has lost popularity in recent years as it has failed to predict the value of the measured flow velocity.

Plyutto *et al.* [5] made the presumption that the jet in a vacuum arc is a plasma stream, and proposed a mechanism for ambipolar acceleration of ions by an electron density gradient based on three extremely revealing experiments. They confirmed the previously known ion velocities, and also showed that there is little or no variation in the velocity of the streams at different angles (θ) from the arc axis in the range $0° < \theta < 60°$, using the angle convention shown in Fig. 1. However, by measuring the mass gain to a series of plates mounted around the arc, they found that while the velocity did not vary with the position, the mass flux in the stream decayed as θ increased.

Their second experiment measured the energy of the ions using a multigrid retarding potential analyzer. They found that the plasma stream contained ions with potentials of up to 70 eV per unit charge for a range of metals including copper. By casting fairly precise shadows behind obstacles in the path of the stream, they ascertained that these high-energy ions could be considered collisionless as they moved away from the cathode spot region.

Finally, using a mass spectroscopic analyzer, they were able to measure the relative population of the ionic species present. They found large numbers of multiply-charged ions (up to +4 for copper).

The results of these last two experiments were combined by the work of Davis and Miller [6] who, by using an electrostatic analyzer in combination with a magnetic analyzer, were able to measure the ion energy distribution of each ionic species, thus leading to a complete ion energy distribution. Their results are now unanimously accepted, and other workers have performed similar measurements on other materials. A complete review of recent ion energy measurements is given in Kutzner and Miller [7]. For the purposes of this paper, we will use the values for copper electrodes from [6]. The measured arc voltage was 20.5 V, the average ion charge was +1.85, and the average ion energy was 89 eV. The most surprising fea-

Manuscript received February 12, 1993. This work was supported by Vacuum Interrupters Ltd. (VIL), England.

The author is with the Department of Engineering Science, Oxford University, Oxford, Oxon OX1 3PJ, England.

IEEE Log Number 9213486.

ture to all theorists is that a 20 V arc can produce 90 eV ions.

As Plyutto *et al.* [5] found in their first experiment, the ion flux decreases as one moves away from the arc axis. The most widely accepted description of the ion current density j_i [8] is

$$j_i = cIx^{-2}\cos\theta \qquad 0 \le \theta < \pi/2$$
$$j_i = c'Ix^{-2} \qquad \theta \cong \pi/2 \tag{1}$$

where θ is the angle to the arc axis, I is the arc current, and x is the distance to the spot center ($x \ge 1$ mm). c is roughly 0.04, and c' is roughly an order of magnitude less for an arc on copper electrodes.

II. Present Ion Acceleration Theories

As a result of the facts presented here, the theoretical task is to find a model that can explain the highly anisotropic acceleration of ions to high energies against the direction of the overall electric field.

According to Kutzner and Miller [7], there are two main theories presently being used to explain these phenomena. The first is the potential hump (PH) theory, first proposed in [5]. This model assumes the creation of a positive space-charge region very close to the cathode surface, at a higher potential than the anode. Such a region would indeed accelerate positively charged ions away from the cathode. The second theory is known as the gas dynamic (GD) theory. This concept was first proposed by Lyubimov [9], and explains ion acceleration as a result of collisions with the higher velocity electron flux close to the cathode.

Kutzner and Miller [7] have investigated how well these theories match the experimental facts. The PH theory predicts that all ions should be accelerated to the same potential, which is (E_z/Z) ion energy per unit charge. In reality, there are distinct peaks in the ion potential distribution, implying that different ionic charge species are accelerated to different potentials. The conclusion is that the PH theory cannot completely explain the ion acceleration.

The GD theory implies that all of the ions should gain the same kinetic energy, which again is not seen in the experimental results, which show that different ionic charge species gain different energies. As a result of these disagreements with experiment, a number of papers [10]–[14] combine these two concepts to create hybrid models that attempt to match the experimental results.

Qualitatively, none of these models attempts to explain the anisotropic distribution of the ion flux, but even quantitatively, they are unable to explain the high ion energies. In all of these models, the GD mechanism is responsible for the largest proportion of the ion acceleration. For example, the Hantzche [14] model divides the total acceleration force into three components:

1) electric field: 21.5 ± 2%
2) pressure gradient: 35.8 ± 1%
3) electron–ion friction: 42.7 ± 3%.

The pressure gradient is a thermally produced force, the electric field acceleration is due to a potential hump that is created as a result of the pressure gradient, and the electron–ion friction is the GD force. Hence, by this theory, an average copper ion with 89 eV of energy receives 38 eV as a result of momentum exchange with electrons.

It will now be demonstrated that the electrons in the arc do not have enough momentum to provide this amount of acceleration. There is a general result [15] that $I_{\text{ion}} \cong 0.1I_{\text{arc}}$, where I_{ion}, the ion current, represents the ions traveling away from the cathode, and thus a negative contribution to the arc current. Davis and Miller [6] also found that the average ion charge in a copper vacuum arc is $+1.8e$. Thus, we can form an equation representing the ratio of the electron to ion production rate:

$$\frac{n_e v_e}{n_i v_i} \cong 20 \tag{2}$$

where n and v are the electron and ion densities and velocities in the axial direction, respectively. An electron produced by the cathode could acquire an energy as the result of the arc voltage of up to 20.5 eV in a 20.5 V arc. This corresponds to an electron momentum of 2.4×10^{-24} kg m/s. The required ion energy as a result of electron collisions is 38 eV, which for a copper ion corresponds to a momentum gain of 1.2×10^{-21} kg m/s. Using (2), showing that only 20 electrons are produced for every ion, we can see that the electrons are unable to provide enough momentum to accelerate the ions by a factor of 25. This presumes that electrons lose no energy in the ionization process, and also that the momentum transfer is 100% efficient, but we know to the contrary that the electrons arrive at the anode with appreciable velocity, which makes the GD process even less credible.

The result of this calculation forces us to question whether the PH model could ever explain the magnitude and direction of the measured ion flux on its own. However, Kutzner and Miller [7] emphasize that the PH model is insufficient to explain the magnitude of the potentials and energies of the ions. Any potential hump higher than the anode potential would be unstable in a vacuum arc because it would draw a very large neutralizing electron current. For completeness, even though never observed in vacuum arcs, positive space-charge humps near the cathode with potentials higher than the anode have only been observed in low-density, low-current (< 1 A) arcs [16]. In such circumstances, the current against the electric field can be maintained by diffusion across the gap as a result of a large electron density gradient. Such gradients are possible in a gas such as argon because of the abnormally long electron mean free path. These arcs, however, still only display a cathode drop roughly equal to the ionization potential of the conducting gas. Thus, at best, in the case of the vacuum arc, which always has an anode potential higher than the ionization potential, the potential hump concept could only apply enough energy to allow the ions to just escape from the cathode region, but not accelerate them further.

As a result of these theoretical inconsistencies in both the PH and GD models, further models will be developed.

III. An Earlier Electrodynamic Model

Before 1965, when the high-velocity jet was thought to consist primarily of vapor [2], [3], the favored acceleration processes were of electromagnetic origin. Maecker [4], although not specifically working on vacuum arcs, developed the theory of magnetic pumping as a method of producing jets in gaseous arcs at artificial constrictions. The theory is based on the inwardly directed "pinch" force on all charged particles that are carrying current in the same direction as the arc current. This pinch leads to an axial pressure which is proportional to the square of the current [17]. The pressure (force/area) created by the pinch is higher at a constriction than in other parts of the arc column. Due to the resulting pressure gradient, there is mass flow (in both directions) along the arc, away from the constriction. Maecker called this magnetic pumping, and although working mainly with a gas arc on carbon electrodes, he demonstrated axial jets from spots on the cathode. Unfortunately, this mechanism is unable to predict the high measured ion energies for the following reasoning. Northrup [17] performed the calculation of the hydrostatic conversion of inwardly directed pinch forces to axial thrust F_{thrust} in a conductor of constant radius, passing current i. Based on his work, Hague [18] derived the following formula, which is confirmed by Lorrain and Corson [19] and transformed here into SI units:

$$F_{\text{thrust}} = \tfrac{1}{2}(\mu_0/4\pi)i^2 \quad \text{Newtons.} \tag{3}$$

For a copper cathode spot of area 10^{-10} m^2 (according to Daalder's [20] measurement), passing 100 A, (3) gives a pressure above the spot of 5×10^6 N/m^2, which is about 50 atm. Without knowing the precise pressure gradient due to the fact that the pinch pressure decreases as one moves away from the cathode, and knowing neither the magnitude nor variation of ion density, it is impossible to say whether this pressure is capable of producing the high-velocity ions. However, by using the results of Tanberg [2] and Kobel [21], who measured the cathode reaction force as a function of arc current without any knowledge of the size of the arc "footprint," it can be shown that Hague's thrust force is usually about two orders of magnitude too small to explain the cathode reaction force. For instance, in a 32 A arc [2], the measured cathode reaction force is 4.5×10^{-3} N, while (3) predicts a thrust force of only 5.1×10^{-5} N.

While this particular mechanism does not seem to provide enough force, there is still evidence that the acceleration process may be dominated by an electromagnetic force, based on the fact that all electromagnetic forces, in situations free from externally applied magnetic fields, are proportional to the square of the current. As the current per cathode spot is solely a function of cathode material [22], in order to vary the spot current, one must use different cathode materials. One can prepare a set of data points relating ion energy to spot current for a group of different metals in order to find whether the ion acceleration force in the vacuum arc depends on the square of the spot current. Data were used from [5], [6], [23], [24] to test this hypothesis.

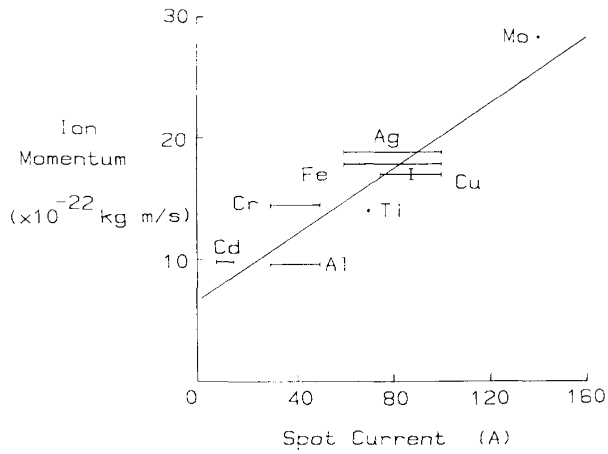

Fig. 2. Ion momentum for eight different metals plotted against the spot current.

The force per unit area which accelerates the plasma above the cathode spot can be considered to be a steady-state momentum flow, which can be expressed as nmv^2, where n is the number density, m is the mass of the particles, and v is their velocity. This can be broken down into $(nv) \times (mv)$, which can be seen to be a momentum flux. If we assume that cathode spots on most metals have similar cross-sectional area, then an electromagnetic force would produce a linear dependence between this momentum flow and the square of the spot current. However, since (nv) represents the ion flux of the plasma, it is proportional to the spot current [15]. It follows that we should examine a possible linear dependence of ion momentum on spot current. The relation between the two is plotted in Fig. 2. The error bars reflect the disparity of measurements between several sets of researchers.

The information in Fig. 2 is not precise enough to deduce that the ion acceleration force definitely depends on the square of the spot current; however, it does at least indicate that ion energies in the vacuum arc are consistent with one of the characteristic signatures of an electrodynamic force.

IV. An Alternative Electrodynamic Model Based on Ampere's Force Law

Fig. 2 demonstrated that an electrodynamic process may provide the solution to the problem of ion acceleration in the vacuum arc, simply because the force on the ions seems to vary as the square of the spot current, that is,

$$F = ki^2. \tag{4}$$

This law of proportionality is applied in the design of many technological applications, ranging from large electromagnets to rail guns. The major difference between the nature of the forces in these devices and in the vacuum arc is that acceleration in the arc occurs in a part of the circuit where the current flows in more or less straight lines. The Lorentz force law predicts no axial force interaction between collinear current elements. However, some recent experiments seem to demonstrate that there can be axial forces and stresses between two portions of a conductor that are in the same straight line.

One of these experiments examines a straight liquid mercury channel between copper bars, and was first performed by Hering [25]. This experiment was repeated by Graneau [26], and is shown schematically in Fig. 3.

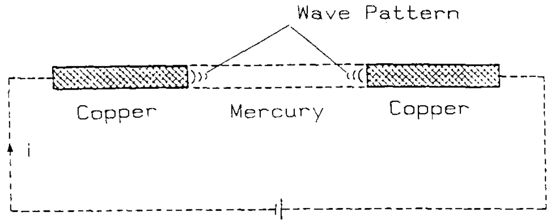

Fig. 3. Schematic diagram of the mercury trough experiment performed in Graneau [25].

The 1/2 in. square copper bars are set into a square groove milled into a plastic board. The space between the bars is filled with liquid mercury to the level of the tops of the bars, so that the continuous current streamlines remain as straight as possible at the copper–mercury interfaces when dc current is flowing, although this experiment works equally well with ac. When 300 A, dc, is passed around the circuit, a wave pattern develops on the surface of the mercury near the interfaces. These patterns only extend a few centimeters into the 20 cm long trough, and appear and disappear virtually instantaneously with the switching on and off of the current. These waves indicate that the liquid is in circulation.

Pinch forces, which compress the channel along its length, cannot account for this circulation as they should not let liquid flow radially outward from the center of the channel at any point along its length. Even more striking is the result that at around 1000 A, the mercury separates from the copper surface at both ends of the channel, causing an arc to form. This causes a current reduction in the circuit, which allows the mercury to flow back onto the copper surfaces again. A continuous series of repeating sparks can be created in this manner. It seems impossible that axial mercury pressure on the copper surface, created by pinch forces, can explain the separation of the whole mercury volume from the surface. All experiments were short enough (1–2 s) to avoid any appreciable temperature increase in the conductors. As this is clearly a current-dependent phenomenon, it provides evidence of an electrodynamic force which can push mass away from a surface in the axial direction. In the vacuum arc, such a longitudinal force would be a means of explaining ion acceleration away from the cathode surface.

Other experiments have not only indicated that these longitudinal forces exist, but have also provided novel and technologically important ramifications [27]. While such forces are not predicted by the normal application of the Lorentz ($\boldsymbol{J} \times \boldsymbol{B}$) force law, they are embraced by what is known as Ampere's force law. The derivation of this law was first published in 1822 [28], but a more condensed version was published in 1825, which has been republished this century [29].

As Ampere knew nothing of electrons or metal lattices, his empirically derived force law is only valid when applied to a current element which is attached solidly to the ions upon which the ponderomotive forces act. When Ampere's law is applied to circuits where the current elements are pieces of conductor with finite length and width, it always produces the correct results. It is suggested by Graneau [30] that a metallic current element can be thought of as an ion on a lattice site, with a finite volume, and local current, with a specific strength and direction. It is in this sense that we are able to apply Ampere's force law to the free plasma ions in the cathode spot.

V. The Ampere Force Formula

The two interacting volume current elements are represented as ($i_m\, dm$) and ($i_n\, dn$), where the i_m and i_n represent the current strengths, and the dm and dn are the characteristic lengths of the elements. The element volumes are always considered to be cubic. This turns out to be important, for otherwise calculations produce meaningless results as there is no control on the number of elements that fill up a given volume. With these definitions in mind, the empirically derived Ampere's force law can be expressed as the force on ($i_m\, dm$) or ($i_n\, dn$) due to interaction with the other element as [27]–[29]

$$\Delta F_{m,n} = -i_m i_n (dm \cdot dn / r_{m,n}^2)(2 \cos \epsilon - 3 \cos \alpha \cos \beta) \tag{5}$$

where $r_{m,n}$ is the distance separating the centers of the two elements, and the angles α, β, and ϵ are defined as shown in Fig. 4.

In (5), a positive sign for ΔF indicates repulsion, and a negative sign attraction. The equal and opposite forces on the two elements always act along the line joining them, thus guaranteeing agreement with Newton's third law. If the currents are in Absolute-Amperes (1 ab-amp = 10 A), then (5) gives the force in dynes (1 dyne = 10^{-5} N). Use of the old electromagnetic units is more convenient for calculation as one can then ignore the ($\mu_0/4\,\pi$) found in the corresponding SI electromagnetic force formula.

Full modeling of the cathode spot in order to calculate the strength and directions of the Ampere forces that might accelerate the ions requires knowledge of the shape of the cathode spot itself, as well as of the configuration of the current streamlines of the primarily electron current flowing from the plasma into the cathode spot and of the current in the cathode itself flowing away from the spot. The

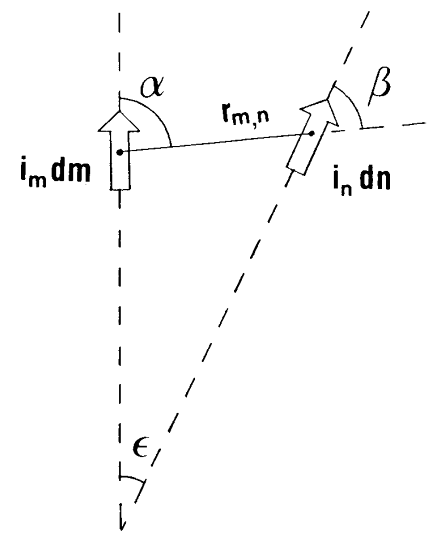

Fig. 4. Angle convention for use with Ampere's force law as expressed in (5).

observation that the plasma moves away from the cathode at a constant flow velocity allows us to assume that the plasma is, in effect, rigid to compression or rarefying forces in the axial direction. This allows us to investigate the separating force between the cathode and the adjacent body of "rigid" plasma by considering only interactions between metal and plasma elements. In this calculation, we are ignoring boundary conditions on the anode side of the plasma, which could have an effect on the force distribution in the plasma block. However, since the plasma is expanding into a vacuum, neglecting the mechanical boundary conditions seems to be justified.

The plasma current element is defined as a fixed finite volume containing one or a group of ions through which flows a current of finite value and direction. Similarly, a metallic element contains one or a group of ions at specific fixed lattice sites with a finite local current. Owing to the inverse square nature of the force law, the separating force pushing the plasma bulk will be mostly due to the current in the metal nearest to it, and the greatest net axial motive force is therefore applied to an ion when it is very near the cathode surface. Because of the Newtonian nature of Ampere's law, no net acceleration of a body of plasma can be achieved by the interaction of elements within it. However, plasma-plasma interactions can explain radial expansion or contraction of the arc column with no effect on the motion of its center of mass, and thus these interactions will only be important when analyzing the angular distribution of forces on individual elements which include the transverse components. The interface across which the axial separating force is calculated is the cathode surface, for the observed effect is a flow of mass away from this division between metal and plasma. The plasma is continuously replenished at the cathode spot as the previously existing ions are pushed away.

VI. The Flat Spot Model

The shape of the cathode spot is most probably that of the crater which remains on the surface after an arc. Daalder [20] has shown that the most likely size of a fully active fast moving spot is approximately 10 μm in diameter. The depth of the crater is a much less regular or well-measured quantity. Thus, the spot shape could be modeled as anything between a hemispherical crater and a flat, circular emitting area. Because of the extra computing complications of a hemispherical crater, only the flat spot will be analyzed.

It was found during calculation with the flat spot model that the accelerating force on a current element according to the Ampere law had dropped by an order of magnitude, less than 1 μm from the cathode surface. It was then realized that a 1 μm layer over a crater of 10 μm diameter could be realistically approximated by a flat spot, especially since the electric field is likely to be normal to the local surface in any case. However, the geometry of the spot is not as important a factor for determining the predictions of Ampere's law as are the directions and densities of current in and out of the cathode/plasma interface. These streamlines will be related to the electric field configurations. Surface irregularities, such as sharp protrusions, may thus have a strong influence on current density and direction, but are not within the input parameters of a first-order computation such as this.

A concave cathode spot in reality appears to be the result of a higher current density near the center of the spot than at the edge. This type of density distribution can be modeled into a flat spot model, although the rate of current decay toward the spot edge can only be very crudely estimated.

For a complete model, there are two distinct regions that need to be described in terms of current patterns: first, the metal of the cathode just below the spot, and second, the plasma zone just above the spot. There are at least three simplistic ways of describing the current patterns in the metal to first order. These are shown in Fig. 5(a)–(c).

Fig. 5(a) is the most likely current pattern from a macroscopic viewpoint with the streamlines diverging radially from a point at the center of the spot. However, in this configuration, the current in some of the elements directly below the spot (which have the strongest effect on the plasma due to the inverse square nature of the force law) is virtually parallel to the metal surface. This cannot be realistic, for the current very near the spot is most likely to be normal to the surface. As a result, this model was not thought to be accurate.

Fig. 5(b) is based on the assumption that the electric field in the metal is axial (vertical), and thus the current streamlines will also be vertical. This model also acknowledges that there must be some divergence of current away from the spot, and thus there are contributions from elements contained in a conical volume below the spot. There is some incompatibility between the requirement of vertical streamlines and a changing cross section. Fortu-

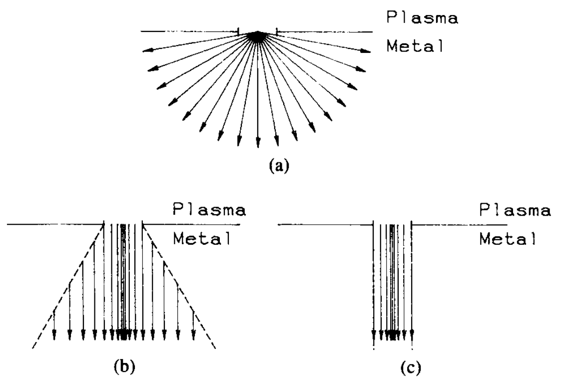

Fig. 5. Possible streamline patterns for the current in the metal cathode in a flat spot model: (a) radial, (b) diverging, (c) vertical.

nately, the resulting current discontinuity errors are greatest for the outermost streamlines, where there is the lowest current density. This assumption stems from the work of Daalder [20], who shows that maximum Joule heating occurs at the center of the spot and decreases towards the edge of the spot. As a result, this was considered a justifiable approximation. Therefore, an important part of this model is a linear fall off in current density toward the edge of the current distribution across any horizontal layer of the conical volume. This means that the force contributions from elements on the edge of the spot are much smaller than those from elements on the spot axis. The current per horizontal slice of this cone, with a semi-angle of 30°, is constant to preserve current continuity.

The third model shown in Fig. 5(c) ignores the effect of the diverging current, and simply considers vertical current streamlines below the spot itself. This too may be fairly realistic because at a given depth in the metal, these elements are the closest to the plasma and pass more current than the outer elements. This model also has the advantage of fewer elements and thus faster computation.

The descriptions of Fig. 5(b) and (c) are both used in the computer simulation, and will be described as the diverging and vertical cathode current cases, respectively.

The plasma region is modeled by using similar ideas. There is a very high axial electric field in the cathode fall region just above the cathode spot surface. Thus, it is again a fair assumption that the current streamlines are vertical in this region. Although the field strength decays rapidly away from the spot, it must still be orientated toward the anode, thus giving no reason to assume anything other than vertical current flow. However, the plasma is usually claimed to be contained in a cone emanating from the cathode spot and having a semi-angle in the region of 30° [3]. Thus, the plasma region has been modeled as such a cone in which the cross-sectional area of the plasma increases away from the cathode spot. This model contains the same current discontinuity as in the diverging current case in the metal [Fig. 5(b)]. However, the argument developed for the cathode metal can again be used to justify the use of vertical current streamlines in a conduction region of changing cross section, as long as the current density is a maximum at the axis.

It has been assumed that current elements both in the plasma as well as in the metal correspond to a cubic volume with a characteristic length which is taken to be the length of one of the sides. The current, which is in the vertical direction, has a value determined by several conditions. First, since the same total current must flow through any layer, the current density must decrease with axial distance from the spot. Second, the current density will not be constant across a given layer, but will have a maximum value at the spot axis. The model was therefore set up so that the ratio of the current in the annulus comprising the outer elements of a layer to that flowing through the central element could be entered as an input parameter. The currents flowing through the inner annuli were calculated by linear interpolation between the two extremes.

Several other numerical inputs were included in the model, such as the number of elements per spot radius and the depth of metal and plasma to be used. This meant that the computation could provide quantitative results which could be compared to experiments. Using Daalder's [20] results for an average copper electrode, the cathode spot was assumed to have a diameter of 10 μm and pass 100 A.

VII. Equations Included in the Model

Calculations of the mutual force between the two current elements using Ampere's force formula requires the cosines of three angles α, β, and ϵ as described in Fig. 4. The formula also contains the distance $r_{m,n}$ between the two elements, as well as the current magnitudes and lengths of the elements. If we use the element length as the unit of distance, and $r_{m,n}$ is calculated in these units, then the $(dm\, dn / r_{m,n}^2)$ term in (5) becomes dimensionless, and the calculated force is dimensionally proportional to the product of the two currents. The obvious choice for the current elements is cubic volumes centered on regularly spaced points on a three-dimensional Cartesian grid. In our calculations, the X and Y axes are parallel to the cathode surface, and the Z axis runs axially through the center of the cathode spot. The results were analyzed by considering the forces in one vertical plane. This was chosen to be the X–Z plane in our calculation. The configuration is shown in Fig. 6.

For these calculations, we select a target element in the plasma with coordinates (d, e, f) and let it interact with other elements (a, b, c). There are various natural constraints on these variables which greatly reduce computing time. For instance, f is always positive since the plasma element must be above the cathode surface. e is always zero because by cylindrical symmetry, only these elements will receive forces in the X–Z plane. d only needs to range over half the diameter because, again by symmetry, the other radius will be the mirror image.

If we taken two typical elements as shown in Fig. 7,

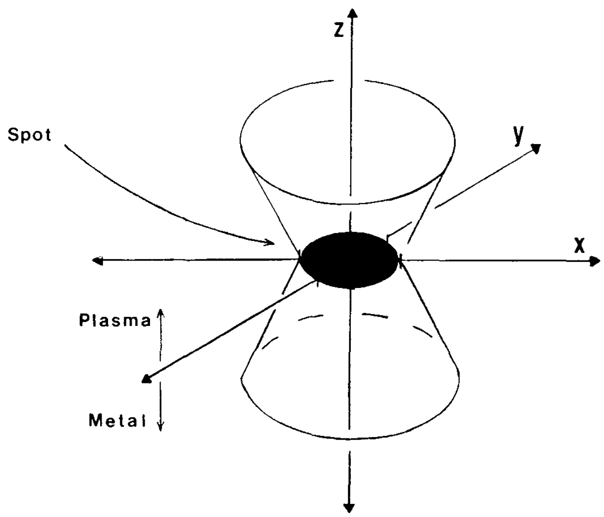

Fig. 6. Axes of flat spot model showing the shapes of the current-carrying regions above and below the spot.

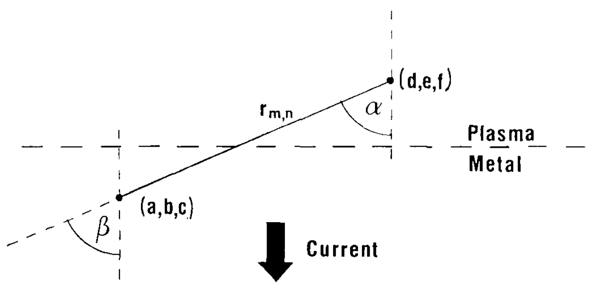

Fig. 7. Two typical current elements and the parameters required to calculate the force between them.

then we can easily calculate the distance $r_{m,n}$ to be

$$r_{m,n} = \sqrt{(d - a)^2 + (e - b)^2 + (f - c)^2}. \quad (6)$$

Since we are assuming that all elements have currents in the vertical direction, then the cosine of the angle between any two is

$$\cos \epsilon = 1. \quad (7)$$

Since the elements are parallel, the angles α and β are equal and can be expressed as

$$\cos \alpha = \cos \beta = \frac{(f - c)}{r_{m,n}}. \quad (8)$$

The final input parameter into the force formula is the current magnitude for each element. The most basic approximation is that the 100 A spot current, passing through any given horizontal layer (parallel to the X–Y plane), is divided evenly among the elements in that layer. This, however, does not represent the physics of the spot adequately, and computation revealed that there was a fairly strong dependence of the results on the current density distribution of a given layer. Daalder [31] has shown that cathode spot operation is dependent primarily on Joule heating, which leads to the probability that the crater center is vigorously heated by this process, while the crater edge is much cooler, relying on thermal conduction from the center to provide enough heat to maintain evaporation and electron emission, although at a reduced rate. If this were not the case, then cathode spots would not be limited to such small sizes. Therefore, the current density at the center of the spot is likely to be much higher than at the edges, and thus for a given horizontal layer, the elements nearer the Z axis pass a higher current than those at the edge.

There is no experimental information to help us decide how the current falls with distance from the spot axis. In order to investigate this issue, each layer was considered to be made up of annular sections of unit element width and height, both in the metal and in the plasma. One of the input parameters in the program was taken to be the ratio of the current in the edge annulus to that in the core element on the axis. All other annuli were then assumed to pass an amount of current that was given by linear interpolation between the outer ring and the core as a function of radius. Although this ratio, called Ω, was fully variable, it was usually taken to be unity for most calculations, implying that all annuli passed the same current, and that the current per element decreased as $1/r$, where r is the distance from the axis.

VIII. Program Structure

The program first selects a particular plasma element, with coordinates (d, e, f) to be used as the target element on which we want to calculate the net force. The height above the cathode surface, again in units of element lengths, determines f. The coordinate e is zero for reasons of symmetry discussed earlier, and d is in the range 0 to X, where X is the number of elements in the radius of the layer. Each target element is allowed to interact with all of the current-carrying elements in the metal, which are identified by the coordinates (a, b, c). The range of these coordinates depends on the choice of the diverging or vertical cathode current models. After each interaction, the force (which is always in the direction of the line joining the elements, and represents repulsion if the sign is positive) is broken down into a horizontal and vertical component. A running sum of the total horizontal and vertical forces on that element is updated after each interaction. At this stage in the calculation, the vertical force component represents that element's contribution to the separating force between the plasma block and the cathode.

In some cases, it was also desired to find the net force, including horizontal components, on the plasma element. This was achieved by also allowing each plasma element to interact with all of the plasma elements except itself. After all of these interactions have been completed, a net force with a specific direction can be predicted for each target element. The results are presented as a graphical representation of these force vectors. It is too complex a problem for this paper to predict the actual flow patterns which would be produced by these forces, but some discussion will be given to a qualitative interpretation of the results.

It was outlined earlier that the Amperian current element is firmly attached to an ion or group of ions. Thus, the force on an element is also the force on the ion itself. The first result required from the program was the force on an ion in the central element, which is where the current per element and net forces are largest, and by symmetry are always directed along the direction of the Z axis. The force on the element F_{e1} can be used as in (9) to find the force on an ion F_i, where v_{e1} is the volume of the element and n_i is the ion density:

$$F_i = \frac{F_{e1}}{v_{e1} n_i}. \tag{9}$$

The volume of the element can be calculated from the 10 μm spot diameter and the number of elements per spot radius. The ion density in the center of the spot is a very troublesome parameter, and rather than insert a value at this stage, it seems more appropriate to calculate the force per unit volume, and then find whether measured ion velocities are predicted with plausible values for the ion density.

IX. Results of the Calculations

The simpler of the two cathode current models is the vertical current case described by Fig. 5(c). For the first set of calculations, concerning forces only on the central element, the difference in results between the diverging and vertical current cases was not enough to warrant the longer computing time for the diverging current model. Therefore, this set of calculations was performed with the vertical current distribution. All results were taken with the semi-angle of plasma divergence equal to 30°. For these calculations, the edge/center current ratio Ω was taken to be unity.

Using this simplified model, the three following general properties can be investigated.

1) How the force on an element depends on the depth of the cathode metal used in the calculation.

2) How the force on an element decays with its distance from the cathode surface.

3) Whether the calculated forces can explain the experimentally observed high ion velocities.

X. Force on an Element as a Function of Cathode Depth Used

By setting the spot radius at five elements and the ratio Ω at unity, the separating force per unit volume at the center of the spot was calculated when elements to different depths of the cathode metal were used. The target element was the central element of the first, second, and tenth plasma layers. These plasma layers are one element in thickness, and the first is the closest to the cathode. By symmetry, the net forces on axial elements must be purely

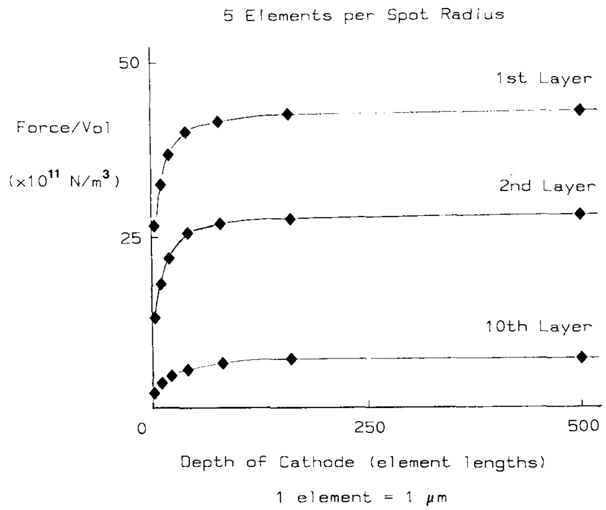

Fig. 8. Vertical force per unit volume on the central element of the first, second, and tenth plasma layer as a function of the depth of cathode metal used in the calculation.

axial. It was explained previously that due to their Newtonian nature, plasma–plasma interactions cannot contribute to the net axial acceleration of the assumed "rigid" plasma block. Thus, in the case of calculating forces on elements in the block that contribute to the block separating from the cathode surface, only plasma–metal interactions are considered. The results of these calculations are presented in Fig. 8.

This figure shows that the effect of the metal on plasma elements decreases as these elements are further from the cathode surface. It also demonstrates that force calculations achieve reasonable accuracy when the cathode depth used is only 20 times the spot radius, which corresponds to a depth of about 0.1 mm. The three curves show that the elements in the first layer (closest to the cathode) receive the most separating force, and that the force on them is also the most dependent on the cathode depth used in the calculation. This is a consequence of the close proximity of this layer to the cathode, and the fact that the force law varies as the inverse square of distance.

This computation also reveals the percentage of the total force on an element due to the first five layers of cathode elements. For plasma layers 1, 2, and 10, this was 62, 48, and 35%, respectively. Again, this highlights the importance of the short distance interactions between the elements nearest the metal/plasma interface. Since the current in this region of high electric field near the interface is likely to be vertical, this is one of the primary justifications for the choice of vertical current streamlines throughout the whole spot model.

XI. Force on an Element as a Function of Distance from the Cathode

The next calculation relates specifically to the decrease in force on the central ions with distance from the cathode spot, indicated by the decrease in the force on elements in successive plasma layers as shown in Fig. 8. The results from this calculation, where cathode current elements are used to a depth of 0.1 mm, are shown in Fig. 9.

Fig. 9 shows that the calculated force per unit volume initially decays even more slowly than $1/r$, where r is the distance from the cathode surface. However, by about 30 μm away from the surface, the force is decaying faster than $1/r^2$. It might be expected that the rate of decay should tend to $1/r^2$ as Ampere's force law (5) is an inverse square law. The reason for this even more rapid decay is that less and less of a proportion of the total current flows through the central element as the radius of the conduction zone expands with height above the spot, so the component $(i_m i_n / r^2_{m,n})$ decreases faster than $1/r^2$. The cause for the initial slow decay of force with distance is slightly more complicated. It is due to the angle function in (5). If we assume that $\epsilon = 0°$, then if $-35.26° < \alpha < 35.26°$ or $144.74° < \alpha < 215.26°$, the angle function is negative and the force between the elements is positive, representing repulsion. However if α falls outside these ranges, the force is attraction. As a result, the interactions of a plasma element near the surface of the metal with some metallic elements can produce significant attractive (downward) forces on the element. A smaller percentage of cathode elements fall in this category for successively higher target elements, and thus the effect of this downward force component decreases. Nevertheless, it causes the reduced initial rate of decay of force observed in Fig. 9.

In reality, the high-density plasma of the cathode spot probably only extends to a distance on the order of the spot diameter ($\simeq 10$ μm). Thus, points on Fig. 9 beyond 10^{-5} m probably have little physical meaning, but nevertheless show that the calculation is plausible.

The three curves on Fig. 9 correspond to different numbers of elements making up the spot radius. As observed, the solution for the separating force per unit volume increases as the number of elements used in the calculation increases. This occurs because we are calculating the force on the central element, and increasing the number of elements necessarily involves continuously clipping off the outer edges of this central element. Because the current falls away from the spot axis, these extremities contributed the least force per volume to the original element, and thus the force per unit volume is increased.

As it is not clear from Fig. 9 how this increase in force per unit volume with increasing X, the number of elements per radius, leads to a value of real physical meaning, another calculation was performed, the results of which are displayed in Fig. 10. Three distances from the cathode surface were selected, namely, 0.5, 2.5, and 64 μm. The same calculation as shown in Fig. 9 was performed, except that different numbers of elements per spot radius (X) were used.

The three curves in Fig. 10 show a steady increase with no apparent limit. This, at first sight, appears to indicate that Ampere's law predicts infinite forces if we let the current element get infinitely small, which is meaningless since we are talking about the force acting on an ion which has finite volume. The paradox here concerns the physical conception of the current element. This topic is discussed in [30], with the conclusion that the ultimate size of a true Amperian current element is defined by the individual ion

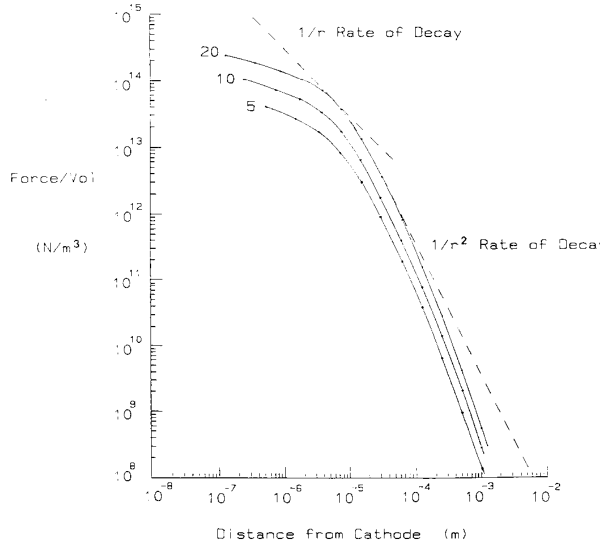

Fig. 9. Vertical force per unit volume on the central plasma elements as a function of distance from the cathode surface. The number next to each curve is the number of elements per radius X.

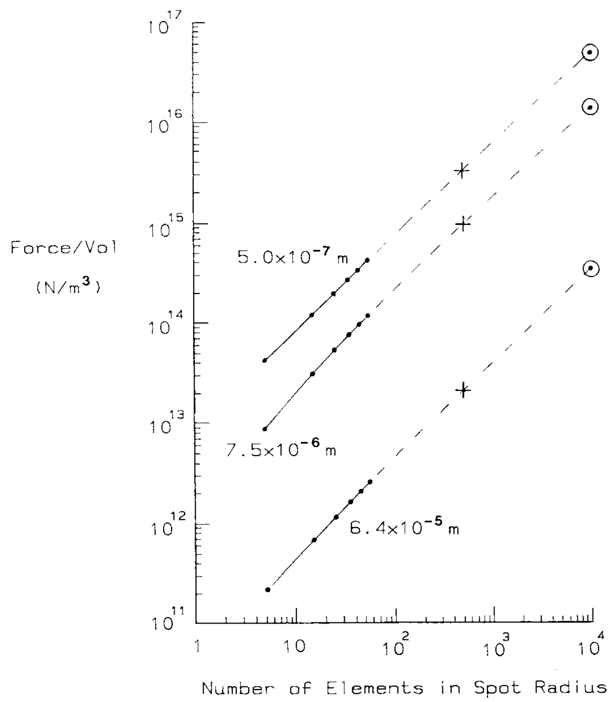

Fig. 10. Vertical force per unit volume on the central axis at three different heights above the cathode spot as a function of number of elements per radius X.

and its enclosing volume. By knowing the ion density, one could determine the true physical element length ($n^{-1/3}$), and thus the number of actual physical elements per spot radius. At a density equal to that of solid copper, this gives 10,000 elements per spot radius, and the extrapolation of the curves in Fig. 10 to the drawn circles gives physical estimates for the force per ion. In fact, the ion density will not be that high, and thus the real forces will be lower than indicated by the circles.

XII. Calculation of the Final Velocity of the Ion

Smeets [32] has shown that the ionization layer is no closer to the cathode than 10^{-8} m. Therefore, we do not need to predict forces on elements within that distance of the surface where there are few ions. With an element length of 10^{-8} m, there are 500 elements per spot radius. The force on the central element can be read from the extrapolations on Fig. 10, marked (+).

These three points are then plotted on Fig. 11, and can be used to extrapolate backwards to find the vertical force per unit volume at 10^{-8} m from the cathode, which comes to 7.5×10^{15} N/m^3.

Fig. 11 can be used to make an estimate for the final velocity of an ion as it is pushed through this varying force region. The one-dimensional motion equation is

$$\int_{10^{-8}}^{10^{-5}} F\, ds = \int_0^U mv\, dv \qquad (10)$$

where 10^{-8} to 10^{-5} m is the distance range of the ion in the cathode spot. 10^{-5} m is considered a sufficient distance from the cathode surface because the force there has dropped by two orders of magnitude, and also it is roughly the spot diameter, making the spot plasma a hemispherical volume. U is the final velocity of the ion after it leaves the spot, v its instantaneous velocity, F the force acting on it, s the distance from the cathode, and m the mass of the ion. Since we only have calculated results for nF, where n is the ion density, (10) may be rewritten as

$$\int_{10^{-8}}^{10^{-5}} nF\, ds = nm \int_0^U mv\, dv. \qquad (11)$$

On the left-hand side of (11), n is included inside the integral because it is also a function of s, the distance from the metal surface, owing to the divergence of the spot plasma as it expands into the vacuum above the cathode. The upper curve on Fig. 11 uses the extrapolated points from Fig. 10, and thus represents the force per unit volume, assuming the same density at the center of layers at all heights above the surface. However, to first order, the relative density at a certain height should be proportional to the density adjacent to the cathode surface by a factor (a^2/b^2), where a is the spot radius (5 μm) and b is the radius of the plasma disk at the required height. Knowing that the semi-angle of plasma dispersion is 30°, we can adjust the upper curve on Fig. 11 for the varying density as shown by the lower curve.

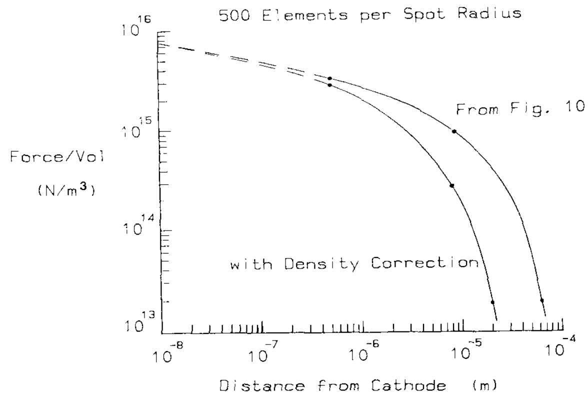

Fig. 11. Vertical force per unit volume on a central element as a function of distance from the cathode, with and without correction for density variation with distance from the cathode.

The calculation to integrate nF was performed numerically from the corrected curve, by application of Simpson's rule, using a step width of 10^{-7} m. Equation (11) then gives

$$\int_{10^{-8}}^{10^{-5}} nF\, ds = 6.1 \times 10^9 \text{ J/m}^3 = \tfrac{1}{2} nmU^2. \qquad (12)$$

By substituting the mass of a copper ion (1.0×10^{-25} kg) for m, we get

$$nU^2 = 1.2 \times 10^{35} \text{ m}^{-1} \cdot s^{-2} \qquad (13)$$

where n is now the density directly adjacent to the cathode surface.

Recently, Anders *et al.* [33] have measured the plasma density in the active regions of the cathode spot to be (3-6) $\times 10^{26}$ m^{-3}. Using this value in (13) produces an ion velocity of (1.4–2) $\times 10^4$ m/s. This agrees very well with the results of a consensus of authors using copper electrodes yielding (1–2) $\times 10^4$ m/s [7]. Thus, this calculation appears to be consistent with the high-ion velocities which have proved to be very difficult to explain in the past.

At this stage, no mention has been made of the charge state of the ion, and how the charge Z might affect the force acting on it. The different velocity distributions of ions with different charge states was highlighted in [6]. This point ultimately requires an even more precise definition of the Amperian current element, which we are not yet in a position to propose. However, since most of the current in an elemental volume is actually carried by electrons, an ion with a certain velocity will only make a small and probably negative contribution to the total element current. The charge on the ion will make a large difference to the ion current in the element, but only a small difference to the total element current. Thus, in determining the force on an element, the ion charge has a small, but nevertheless noticeable effect. However, a better understanding of this point would also require a more thorough calculation, taking into account the velocities and charges of each ion so that the ion current fraction for each element could be included. It would also be useful to have some knowledge of whether all ionization occurs at nearly the same distance from the cathode, or whether different charge states are formed in different regions. Nevertheless, the Ampere solution seems to provide a conceivable mechanism by which the ions of different charge state Z acquire slightly different velocities.

XIII. Spatial Analysis of Forces on the Plasma of the Cathode Spot

For these calculations that took into account all element interactions, there was a noticeable difference in the results between the vertical current and diverging current cases [Fig. 5(b) and (c)], so both of these were explored, and it was concluded that the diverging current case was more realistic, and subsequently used exclusively. The net force on each plasma element in the cathode spot dispersion cone was calculated as described earlier. Again, the fluid mechanical problem of deducing velocities has not been attempted, but a map has been constructed of the strength and directions of forces on elements in a plane which includes a diameter of the cathode spot. Due to cylindrical symmetry, all of the forces on these elements are in the same plane as well.

A plot is shown in Fig. 12, which shows only half of the area above the cathode spot, with the spot axis on the left. The directions of the arrows represent the force direction, and the length of the arrow base is proportional to the force magnitude. The predominance of force vectors pointing primarily toward the axis is representative of the pinch force which is known to exist in any current distribution. However, the important feature which distinguishes these predictions is the axial electromagnetic forces that occur at and near the arc axis, which would result in axial ion acceleration.

For this calculation, it was decided that the most realistic current density distribution is represented by $\Omega = 1$. In this situation, the axial forces are larger than the simultaneous pinch forces, and they tend to a constant magnitude with distance from the cathode. In future work on the fluid dynamical consequences of this force map, this constant force along the axis may be very helpful, and it adds strength to the assumption that the plasma moves as a rigid block. One must presume that ions found at angles closer to the cathode plane have been deflected by secondary effects such as a glancing collision, or electrostatic repulsion from other ions or from the anode.

XIV. Retrograde Motion

This suggested method of ion acceleration, by longitudinal forces, would not require changes to any of the present theories concerning spot formation. However, it is possible that the explosion of microprotrusions is the result of electrodynamic longitudinal forces rather than the thermal effects normally proposed. It was claimed in [34] that the behavior of a microprotrusion was like an exploding wire, and it is shown in [35] that the fracture

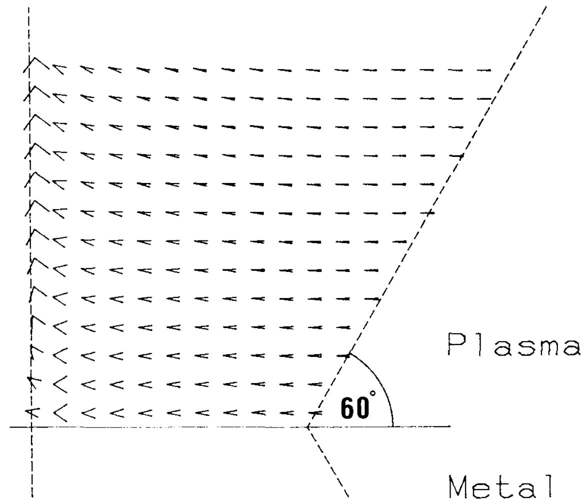

Fig. 12. Map of forces on plasma current elements over half the cathode spot, with the axis on the left. The force magnitude is proportional to the length of the arrow base, and is applied in the direction of the arrow.

of these wires can be explained by the electrodynamic longitudinal forces derived from Ampere's law. Whether they break by electrodynamic or thermal forces is likely to depend on the rise time of the current pulse. Nevertheless, the rest of the present cathode spot theory concerning particle evaporation by ohmic heating and the consequent ionization of these neutral atoms remains consistent with longitudinal accelerating forces.

However, there is possibly a new mechanism for macroparticle emission, and also retrograde spot motion, that follows as a consequence of using Ampere's force law as the ion acceleration mechanism. A feature of the longitudinal Ampere force is that a current element in the metal that accelerates another in the plasma receives an equal and opposite reaction force. This means that the cathode reaction force will always be precisely equal and opposite to the force accelerating the plasma jet. Thus, there should be a strong downward force on the thin layer of molten metal between the solid metal and the plasma, due to its close proximity to the interacting plasma. This force is capable of hydrostatically squeezing the molten material across the surface and out of the sides of the cathode crater. Such material is usually detected in droplet form, and it can be understood why it is ejected at angles within 30° of the cathode plane [36]. Some of these droplets inevitably are ejected so close to the cathode plane that they soon hit cooler metal and solidify, forming a raised ridge around the crater, as is shown by all visual observations of cathode spot craters [8].

An attractive feature of this proposed mechanism is a possible explanation of retrograde spot motion. The highly mobile plasma electrons which carry most of the arc current are subject to the conventional deflecting forces due to the magnetic field parallel to the cathode surface, caused by other spots or external magnets. This then causes the plasma current channel to be slightly bent in

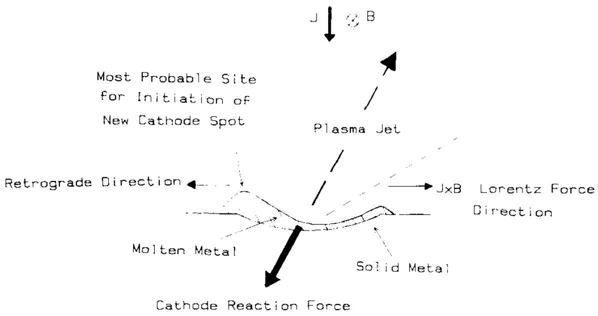

Fig. 13. Diagram of proposed mechanism of cathode spot retrograde motion.

the Lorentzian direction, as has always been observed [37]. The corresponding equal and opposite reaction force on the cathode, predicted by the Ampere force law, must now be mainly downward, but with an extra component in the retrograde direction. This force, acting on the molten metal in the crater, will force more of the material out of the retrograde side of the spot, thus building up the rim on the retrograde side of the crater with respect to the other crater edges. As Rakhovskii [38] points out, spot initiation usually occurs at the rim of the previous crater. Thus, an increased height of the rim on the retrograde side of the spot leads to an increased chance for the next spot to be initiated there. This can then lead to spot motion in the retrograde direction. This process is depicted in Fig. 13. Drouet [39] presents evidence that dielectric barriers on the cathode surface stop the arc when in retrograde motion, but only delay it in Lorentzian motion. This fact is consistent with the Ampere model, which implies that retrograde motion relies on the metal surface, while Lorentzian motion has more to do with the plasma channel being bent by the magnetic forces.

XV. Conclusions

It has been shown earlier that for $\Omega = 1$, the axial forces computed from Ampere's force law are apparently capable of predicting the observed high-ion velocities in the direction toward the anode. Although it has not been fully demonstrated that the force diagram of Fig. 12 leads to the previously discussed anisotropic ion density, it can be seen from the force diagrams that since there are strong axial forces, there will be a predominance of ions being accelerated in the vertically upward direction. However, a full solution would be a difficult problem beyond the scope of this paper. Nevertheless, an acceleration mechanism has been outlined that appears to predict some of the most anomalous cathode spot behavior, while remaining consistent with all of the accepted cathode spot facts concerning current density, spot motion, and cathode reaction force.

An Amperian force in the direction of current flow, with balanced action and reaction, seems to provide an explanation for phenomena which have been missing from the previous theories advanced for the remaining enigmas of cathode spot behavior. While such a force does not interfere with the particle production processes, which have been fairly well established for some time, it appears to explain the high-energy ion acceleration process, which has been an acknowledged mystery since these ions were first discovered. It can also shed new light on macroparticle emission, and in doing so, seems to yield one of the least contrived explanations of retrograde motion.

Acknowledgment

This paper represents some of the work in the author's D. Phil. dissertation [40], where more details of the complete calculation can be found. The author would like to thank Dr. A. M. Howatson for his help and advice throughout this work.

References

[1] P. Malkin, "The vacuum arc and vacuum interruption," *J. Phys. D: Appl. Phys.*, vol. 22, pp. 1005–1119, 1989.
[2] R. Tanberg, "On the cathode of an arc drawn in vacuum," *Phys. Rev.*, vol. 35, pp. 1080–1089, 1930.
[3] M. P. Reece, "The vacuum switch: Part 1—Properties of the vacuum arc," *Proc. IEE*, vol. 110, no. 4, pp. 793–802, 1963.
[4] H. Maecker, in *An Introduction to Discharge and Plasma Physics*, S. C. Haydon, Ed. Univ. New England, Armidale NSW, Australia, 1964, Ch. 20, pp. 245–265.
[5] A. A. Plyutto, V. N. Ryzhkov, and A. T. Kapin, "High speed plasma streams in vacuum arcs," *Sov. Phys.—JETP*, vol. 20, no. 2, pp. 328–337, 1965.
[6] W. D. Davis and H. C. Miller, "Analysis of the electrode products emitted by dc arcs in a vacuum ambient," *J. Appl. Phys.*, vol. 40, no. 5, pp. 2212–2220, 1969.
[7] J. Kutzner and H. C. Miller, "Ion flux from the cathode region of a vacuum arc," *IEEE Trans. Plasma. Sci.*, vol. 17, no. 5, pp. 688–694, 1989.
[8] B. Juttner, "Characterization of the cathode spot," *IEEE Trans. Plasma. Sci.*, vol. PS-15, no. 5, pp. 474–480, 1987.
[9] G. A. Lyubimov, "Dynamics of cathode vapor jets," *Sov. Phys. Tech. Phys.*, vol. 22, no. 2, pp. 173–177, 1977.
[10] L. P. Harris, "A mathematical model for cathode spot operation," in *Proc. VIIIth Int. Symp. Discharges and Elec. Insul. in Vacuum*, Albuquerque, NM, 1978, paper F1, pp. 1–18.
[11] B. Ya Moishes and V. A. Nemchinskii, "Erosion and cathode jets in a vacuum arc," *Sov. Phys. Tech. Phys.*, vol. 25, pp. 43–48, 1980.
[12] C. Wieckert, "The expansion of the cathode spot plasma in vacuum arc discharges," *Phys. Fluids*, vol. 30, no. 6, pp. 1810–1813, 1987.
[13] V. L. Sizonenko, P. I. Markov, L. I. Kiselevskii, and G. G. Shergin, "Buneman instability in an arc cathode spot," *Sov. Phys. Tech. Phys.*, vol. 29, no. 11, pp. 1259–1263, 1984.
[14] E. Hantzche, "A simple model of diffuse vacuum arc plasmas," *Contrib. Plasma Phys.*, vol. 30, no. 5, pp. 575–585, 1990.
[15] C. W. Kimblin, "Erosion and ionization in the cathode spot regions of vacuum arcs," *J. Appl. Phys.*, vol. 44, no. 7, pp. 3074–3080, 1973.
[16] K. T. Compton and C. Eckart, "The diffusion of electrons against an electric field in the non-oscillatory abnormal low voltage arc," *Phys. Rev.*, vol. 25, pp. 139–146, 1925.
[17] E. F. Northrup, "Some newly observed manifestations of forces in the interior of an electric conductor," *Phys. Rev.*, vol. 24, pp. 474–497, 1907.
[18] B. Hague, *Electromagnetic Problems in Electrical Engineering*. London: Oxford Univ. Press, 1929, p. 347.
[19] P. Lorrain and D. R. Corson, *Electromagnetism, Principles and Applications*. W. H. Freeman and Co., San Francisco, p. 326 (1978).
[20] J. E. Daalder, "Diameter and current density of single and multiple cathode discharges in vacuum," *IEEE Trans. Power App. Syst.*, vol. PAS-93, pp. 1747–1758, 1974.
[21] E. Kobel, "Pressure and high velocity vapour jets at cathodes of a mercury vacuum arc," *Phys. Rev.*, vol. 36, pp. 1636–1638, 1930.
[22] B. E. Djakov and R. Holmes, "Cathode spot division in vacuum arcs

with solid metal cathodes," *J. Phys. D: Appl. Phys.*, vol. 4, pp. 504–509, 1971.

[23] L. P. Harris, in *Vacuum Arcs, Theory and Application*, J. M. Lafferty, Ed. New York: Wiley, 1980, ch. 4.

[24] V. M. Lunev, V. G. Padalka, and V. M. Khoroshikh, "Plasma properties of a metal vacuum arc II," *Sov. Phys. Tech. Phys.*, vol. 22, no. 7, pp. 858-861, 1977.

[25] C. Hering, "Electromagnetic forces; A search for more rational fundamentals; A proposed revision of the laws," *AIEE J.*, vol. 42, pp. 139-154, 1923.

[26] P. Graneau, "Ampere tension in electric conductors," *IEEE Trans. Magn.*, vol. MAG-20, pp. 444-455, 1984.

[27] —, *Ampere-Neumann Electrodynamics of Metals*. Palm Harbor, FL: Hadronic, 1985.

[28] A. M. Ampere, "La determination de la formule qui represente l'action mutuelle de deux portions infiniment petites de conducteur voltaiques," L'academie Royale des Sciences, Paris, 1822.

[29] —, *Theorie Mathematique des Phenomenes Electro-Dynamiques Uniquement Deduite de L'experience*. Paris: Blanchard, 1958.

[30] N. Graneau, "The finite size of the metallic current element," *Phys. Lett. A*, vol. 147, no. 2, 3, pp. 92-96, 1990.

[31] J. E. Daalder, "Cathode spots and vacuum arcs," *Physica*, vol. 104C, pp. 91-106, 1981.

[32] R. P. P. Smeets, "Low-current behaviour and current chopping of vacuum arcs," Ph.D. dissertation, Eindhoven Univ. Technol., 1987.

[33] A. Anders, S. Anders, B. Juttner, W. Botticher, H. Luck, and G. Schroder, "Pulsed dye laser diagnostics of vacuum arc cathode spots," *IEEE Trans. Plasma. Sci.*, vol. 20, no. 4, pp. 466-472, 1992.

[34] J. Rothstein, in *Exploding Wires, Vol. 3*, W. G. Chace and H. K. Moore, Ed. New York: Plenum, 1964, pp. 115-123.

[35] P. Graneau, "First indication of ampere tension in solid electric conductors," *Phys. Lett. A*, vol. 97, pp. 253-255, 1983.

[36] J. E. Daalder, "Components of cathode erosion in vacuum arcs," *J. Phys. D: Appl. Phys.*, vol. 9, pp. 2379-2395, 1976.

[37] A. E. Robson and A. Von Engel, "Motion of a short arc in a magnetic field," *Phys. Rev.*, vol. 104, pp. 15-16, 1956.

[38] V. I. Rakhovskii, "Experimental study of the dynamics of cathode spot development," *IEEE Trans. Plasma. Sci.*, vol. PS-4, no. 2, pp. 81-102, 1976.

[39] M. G. Drouet, "The physics of the retrograde motion of the electric arc," *IEEE Trans. Plasma. Sci.*, vol. PS-13, no. 5, pp. 235-241, 1985.

[40] N. Graneau, "Ion dynamics of diffuse vacuum arcs," D. Phil. dissertation, Oxford Univ., Oxford, England, 1992.

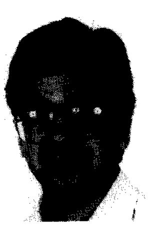

Neal Graneau was born in London, England, on July 3, 1963. He spent several summers working on fundamental electromagnetism at MIT, Cambridge, MA, while attending high school in the U.S. After a year working on far-infrared spectroscopy at Imperial College in London, he received the B.Sc. degree in physics from King's College, London, in 1986. After receiving the M.Sc. degree in the science and applications of electric plasmas from Oxford University in 1987, he continued his research there on ion acceleration mechanisms in vacuum arcs for the D.Phil. degree, which he received in 1992.

He is still at Oxford University, working in the Pulsed Power and Applications Group, and has been studying high-voltage transmission line transformers and exploding wires.